

# Fast Lifetime Blinking in Compact CdSe/CdS Core/Shell Quantum Dots


Published as part of *The Journal of Physical Chemistry* virtual special issue “125 Years of *The Journal of Physical Chemistry*”.

Yonglei Sun, Hua Zhu, Na Jin, Ou Chen, and Jing Zhao\*

 Cite This: *J. Phys. Chem. C* 2021, 125, 15433–15440

 Read Online

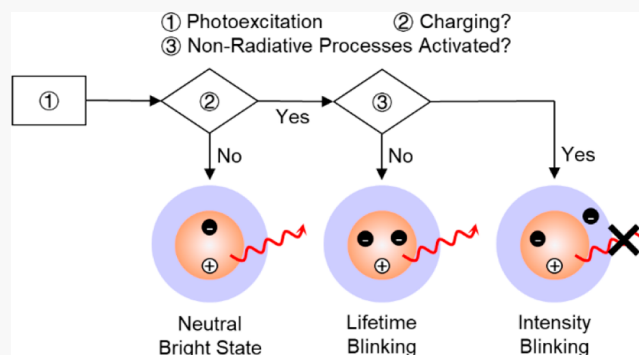
ACCESS |

 Metrics & More

 Article Recommendations

 Supporting Information

**ABSTRACT:** Lifetime blinking is another type of fluorescence fluctuation in single colloidal quantum dots (QDs) apart from the extensively studied intensity blinking. It is a phenomenon of fluctuations in the fluorescence lifetime of a single QD over time while its fluorescence intensity is relatively unaffected. So far lifetime blinking has only been reported in a few QD systems, such as “giant” (i.e., thick-shell) CdSe/CdS core/shell QDs. It remains unclear whether this phenomenon is universal among QDs. In this work, we use statistical methods to demonstrate that the lifetime blinking state, although short-lived, also exists in compact CdSe/CdS core/shell QDs in which nonradiative processes are efficient and lead to intensity blinking when activated. We propose that lifetime blinking happens when a negative trion forms in the core of a QD after photoexcitation while nonradiative processes are not activated. However, the easy accessibility to efficient nonradiative processes results in the short durations of lifetime blinking events in this type of QDs.



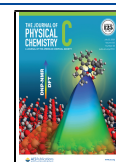
## INTRODUCTION

A mechanistic understanding of the photophysical properties of colloidal quantum dots (QDs) is the essential step toward unleashing QDs' full potential in various real-world applications. A characteristic photophysical property of single QDs is the fluorescence intensity intermittency, or intensity “blinking”, under continuous illumination. Intensity blinking has been under the spotlight for decades since its discovery.<sup>1</sup> Lifetime blinking is another type of fluorescence fluctuations observed in QDs. It describes the switch of fluorescence lifetime of a single QD between two distinct levels while the fluorescence intensity of the QD is largely unaffected.<sup>2</sup> The longer lifetime is assigned to the photoluminescence (PL) lifetime of neutral excitons (bound electron–hole pairs), whereas the shorter one, whose value is about half of the longer one, is assigned to the PL lifetime of charged excitons (also known as “trions”). Lifetime blinking was first observed in “giant” CdSe/CdS QDs with thick shells (~15 monolayers),<sup>2</sup> then in CdSe/CdS QDs with multiple radially graded interfacial alloy layers<sup>3</sup> and InP/ZnSe/ZnS core/multishell QDs.<sup>4</sup> The discovery of lifetime blinking challenges the commonly accepted relationship between charging and intensity blinking. Previously, charging in QDs was considered to be responsible for the less bright intensity states,<sup>5</sup> though the exact mechanism is still unclear. Yet the presence of lifetime blinking suggests that charging

does not necessarily lead to intensity blinking. In-depth investigations into lifetime blinking are therefore beneficial to better understand the mechanisms of charging-related fluorescence fluctuations in single QDs. However, contrary to the extensively studied intensity blinking, reports on lifetime blinking of QDs at room temperature are rare to date.

The main cause of the rarity of lifetime blinking studies compared to intensity blinking is likely rooted in the intrinsic differences when analyzing PL lifetime and intensity. Traditional timing analysis methods utilize a binning technique that assigns photons into a series of binning time intervals by their absolute arrival times. The PL intensity of each bin is defined as the number of photons within the bin. By simply relying on photon counting, the PL intensity determination is inherently model-free. Thus, the studies on PL intensity blinking are relatively easy, and fast intensity fluctuation events can be detected by choosing a finer bin time<sup>6</sup> or applying correlation analyses.<sup>7,8</sup> On the contrary, the PL lifetime of each bin is

Received: May 3, 2021  
Revised: June 25, 2021  
Published: July 13, 2021



derived from fitting models, such as exponential decay models, on the microscopic photon arrival times relative to the corresponding excitation pulses. Reliable fitting results depend on a decent size of observables.<sup>9</sup> Unfortunately, fluorescence emission from single QDs is weak, and detection efficiencies of single-photon detectors are limited. Because of that, the bin times used in PL lifetime analyses cannot be arbitrarily small. Consequently, fast PL lifetime fluctuation events whose durations are shorter than bin times are unlikely to be detected. Indeed, all of the QDs reported to exhibit lifetime blinking thus far share a common characteristic: the durations of their lifetime blinking events can be significantly longer than the bin times (typically 50–200 ms) used in analyses. Therefore, lifetime blinking is clearly manifested by two distinct populations of different lifetimes at similar intensities in corresponding fluorescence lifetime-intensity distribution (FLID) plots. Because of the rarity of lifetime blinking studies and difficulties in detecting possible fast PL lifetime blinking events by traditional binning analysis methods, so far it is unclear whether the phenomenon is universal among QDs like intensity blinking or it only exists in specific types of QDs.

Here we choose CdSe/CdS core/shell QDs with  $\sim 6$  monolayers of CdS in the shell as a model system to study the possible lifetime blinking. Synthesized via a well-developed approach,<sup>10</sup> this type of compact core/shell QDs are representative and routinely used in research nowadays; the ensemble PL quantum yield is decent ( $\sim 90\%$ ), yet intensity blinking can still be observed among individual QDs. We utilize statistical methods to demonstrate that lifetime blinking also exists in such QDs. Lifetime blinking could happen when a negative trion forms in the core of a QD after photoexcitation. Depending on whether the nonradiative processes are activated, the charged QD will be in the intensity blinking state or lifetime blinking state, whereas the former is favored in this type of QDs. Even if a lifetime blinking event occurs, it could be quickly terminated by discharging or activation of efficient nonradiative processes. Owing to their short durations, the lifetime blinking events in the compact CdSe/CdS QDs were not detected by traditional binning analysis methods previously.

## EXPERIMENTAL SECTION

High-quality colloidal CdSe/CdS QDs with a moderate shell thickness ( $\sim 6$  monolayers of CdS) were synthesized for this study. Details of the synthesis are described in previous literature<sup>10</sup> and in Supporting Information (SI) Section 1.1. The extinction and PL spectra of QDs are shown in Figure S2 and the QDs have a PL peak at  $\sim 625$  nm. PL of single QDs was excited by a 405 nm pulsed laser at a 2.5 MHz repetition rate. PL signals were spectrally filtered by  $630 \pm 30$  nm bandpass filters and recorded by single-photon counting modules ( $\tau$ -SPAD, PicoQuant) in the time-tagged time-resolved format. PL cross-correlation of single QDs was also measured through a Hanbury–Brown–Twiss setup. All spectroscopic measurements were performed at room temperature. Details of the measurements can be found in SI Section 1.2.

## RESULTS AND DISCUSSION

Figure 1 shows the analyses of the PL signals from a single example QD by traditional binning methods with a 50 ms bin time. The cross-correlation function in Figure 1b shows a

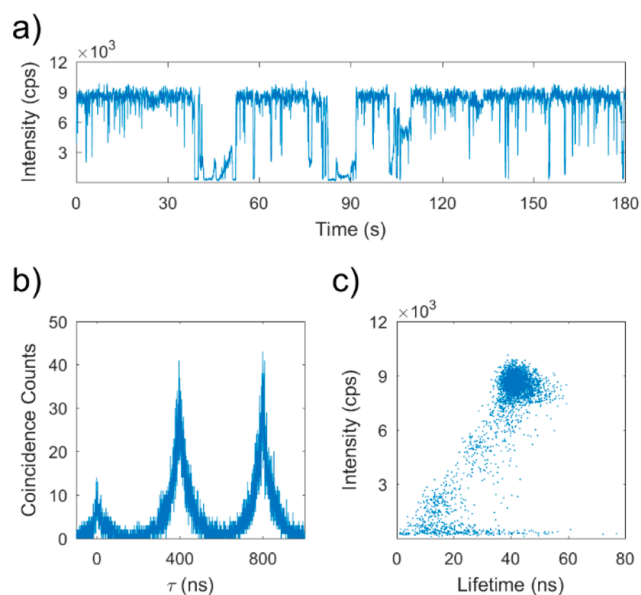


**Figure 1.** Traditional analyses of the PL signals from a representative QD. The bin time is 50 ms. (a) PL intensity trajectory. (b) Cross-correlation function. (c) FLID.

series of peaks with the same time interval as that between the excitation pulses (400 ns). The zero-delay time peak ( $\tau = 0$ ) is much smaller compared to other peaks. This clear antibunching feature<sup>11</sup> proves that the PL signals came from a single QD. The PL intensity trajectory in Figure 1a shows typical distinct intensity blinking characteristics. The PL quantum yield of the QD is determined by the rates of radiative and nonradiative processes. The less bright intensity levels in the PL intensity trajectory indicate that at some periods, the PL quantum yield of the QD is considerably lower than unity. It means when the nonradiative processes in the QD are activated, their rates are comparable or faster than that of the exciton radiative recombination. The FLID of this QD is constructed (see details in SI Section 2.1) and shown in Figure 1c. Apart from the low-intensity data points possessing unreliable lifetime values, the PL intensity and lifetime of the QD present a general positive correlation. There are no discernible two populations of similar intensities but different lifetimes in the FLID, which is expected for this kind of compact CdSe/CdS QDs. Nevertheless, this observation does not exclude the possibility of lifetime blinking in the QD because, as discussed above, fast PL lifetime fluctuation events are unlikely to be detected via this traditional analysis method.

The main drawback of traditional binning analysis methods is that by assigning artificial time intervals, the analyses produce artifacts<sup>6,12</sup> and are unnecessarily limited by the size of the bin time. On one hand, state transition events may happen in some bins, yet the data within these bins usually are not treated differently; on the other hand, certain consecutive bins may belong to one state, but they are analyzed separately. In order to overcome this drawback and properly group consecutive bins of the same intensity state, change-point analysis<sup>13</sup> is employed here. This analysis method considers a trajectory corrupted by Poisson noise<sup>13</sup> or Gaussian noise<sup>14</sup> as some periods of constant intensity levels linked with sudden transitions. After detecting the intensity change points, the trajectory is divided into a series of segments. Since the bins within one trajectory segment are asserted to be in the same

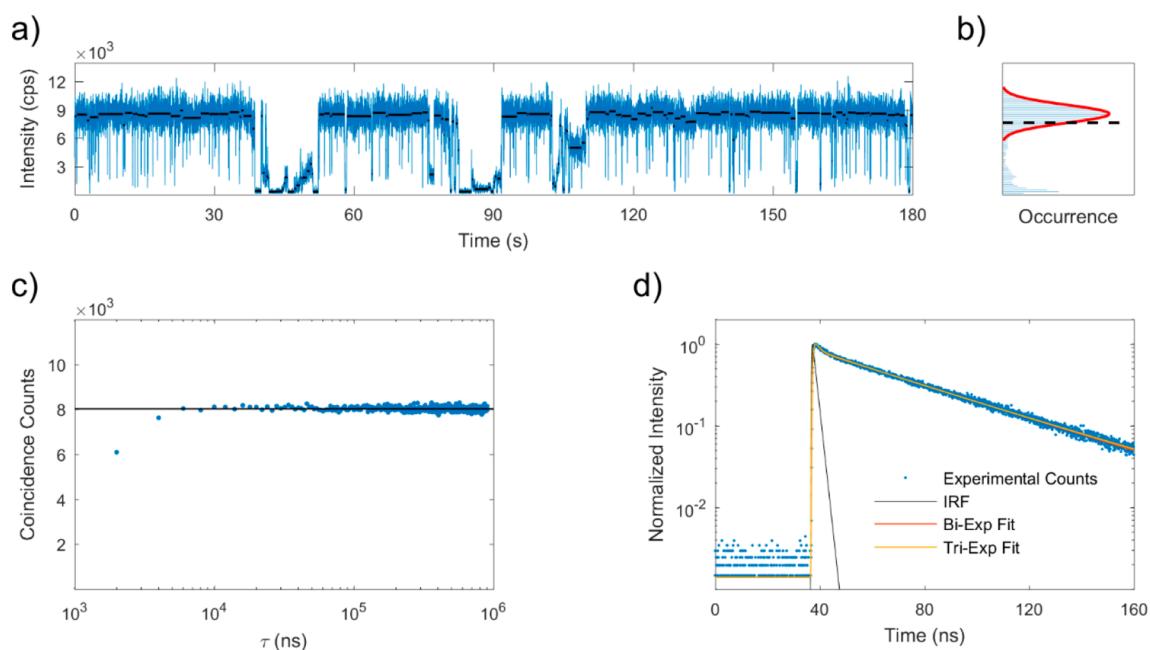


**Figure 2.** (a) Reconstructed intensity trajectory of the same QD (bin time: 10 ms). Black lines denote the trajectory segments identified by the change-point analysis, whose heights represent their mean intensity levels, and lengths represent their durations. (b) Histogram of the intensities from (a). A Gaussian fit of the high intensity counts is represented by the red curve, while the intensity level of one standard deviation below the mean from fitting is represented by the dashed black line. (c) Autocorrelation function of the selected bright intensity trajectory segments. (d) The PL decay curve of the selected bright intensity trajectory segments (blue) is fitted by convoluting IRF (black) with a biexponential decay model (red) or a triexponential decay model (yellow).

intensity state with statistical rigor, they can be analyzed altogether, therefore overcoming the limits of traditional binning analysis methods. In order to detect fast intensity blinking events that last shorter than 50 ms while retaining acceptable signal-to-noise ratio, we choose a 10 ms bin time and reconstruct the PL intensity trajectory of the same example QD. The new PL intensity trajectory is shown in Figure 2a, on which we performed the change-point analysis (see details in SI Section 2.2) developed by Li *et al.*<sup>14</sup> The resultant trajectory segments are plotted as black line segments in Figure 2a, whose heights represent their mean intensity levels, and lengths represent their durations. These trajectory segments, instead of individual bins, are used for the subsequent analyses.

The bright intensity state of QDs is well-defined compared to other intensity states (e.g., “gray” and “off” states). Because of the large number of photons contained in the bright intensity state, its PL lifetimes can be more reliably and accurately determined from fitting, hence ideal for lifetime blinking studies. Here, the trajectory segments of the bright intensity state of the QD are selected by a conservative criterion. Shown in Figure 2b, the high counts of the intensity histogram can be well fitted by a Gaussian function (red curve). We set a threshold (dashed black line) one standard deviation below the mean from the Gaussian fitting, and only select trajectory segments whose mean intensities surpass this threshold. The autocorrelation function  $g(\tau)$  at the microsecond time scale of the selected trajectory segments is calculated and shown in Figure 2c. The value of  $g(\tau)$  is the probability of detecting another photon after a delay time  $\tau$  given a photon is detected multiplied by a constant factor.<sup>15,16</sup> Except for the residue effect of antibunching and periodic excitation near the nanosecond time scale, the autocorrelation values are pretty close to their mean (black line). It means

during the selected trajectory segments, given a photon is detected, the probability of detecting another photon after a microsecond time scale delay time is the same. This observation suggests that there are no fast intensity blinking events during the selected trajectory segments and is consistent with previous literature.<sup>8</sup>

Under a mild excitation condition, spectrally filtered QD PL signals contain photons from band-edge exciton and biexciton recombination because single excitons and biexcitons fluoresce at similar wavelengths.<sup>17</sup> The PL decay curve of the bright intensity state is hence traditionally fitted with a biexponential decay model. If lifetime blinking exists in the bright intensity state, the PL decay curve should be better fitted with a triexponential decay model. In Figure 2d, the PL decay curve of the selected trajectory segments of the bright intensity state is fitted by convoluting instrument response function (IRF) with biexponential or triexponential decay models using maximum likelihood estimation (MLE, see details in SI Sections 2.4 and 2.5)

$$\text{IRF} * \sum_i A_i \cdot e^{-t/\tau_i}$$

where \* denotes convolution. Biexponential decay model fitting gives two lifetime components of 0.74 and 43.16 ns, which are typical values of PL lifetimes of biexciton and exciton for this type of QDs, respectively.<sup>18</sup> Triexponential decay model fitting gives two similar lifetime components of 0.70 ns, 45.67 ns, and an additional lifetime component of 25.60 ns. Intuitively, both models fit the PL decay curve well (see Figure 2d); however, the goodness of fit can be evaluated quantitatively with statistical significance. Note the biexponential decay model is nested within the triexponential decay model, that is, the triexponential decay model has two more

parameters (2 degrees of freedom): an additional lifetime component and its pre-exponential factor. Likelihood ratio test (LRT) can thus be applied to verify at a certain significance level whether triexponential decay model fits better than biexponential decay model. The maximum likelihoods  $\mathcal{L}_{\text{Bi}}$ ,  $\mathcal{L}_{\text{Tri}}$  corresponding to biexponential decay model and triexponential decay model are obtained from the MLE fitting. Then the quantity  $\lambda_{\text{LR}}$  for LRT can be computed by

$$\lambda_{\text{LR}} = -2(\log \mathcal{L}_{\text{Bi}} - \log \mathcal{L}_{\text{Tri}})$$

and compared to a critical value with 2 degrees of freedom at a certain significance level. For the two models fitting the PL decay curve of the selected trajectory segments of the QD,  $\lambda_{\text{LR}}$  is 66.324. At the 0.05 significance level, the most common significance level used in physical sciences, the critical value with 2 degrees of freedom is 5.991. This critical value is considerably smaller than the calculated  $\lambda_{\text{LR}}$ . LRT assesses that at the 0.05 significance level, the triexponential decay model better fits the PL decay curve than the biexponential decay model. This is a strong indication of lifetime blinking in the selected trajectory segments since the additional lifetime component cannot come from the emission of other QDs or during the periods of the QD's other intensity states as demonstrated above.

Now we look into individual selected trajectory segments. Figure 3a shows an episode of the PL trajectory of the example QD along with change-point analysis results. The trajectory segment highlighted by the red line is a segment selected as in the bright intensity state for PL lifetime analysis. This trajectory segment contains 7951 photons, and its duration is 0.98 s. The corresponding PL decay curve shown in Figure 3b is analyzed by the same recipe described above. MLE fitting of the biexponential decay model gives two lifetime components of 0.62 and 38.77 ns, whereas the triexponential decay model fitting gives two similar lifetime components of 0.47 ns, 46.04 ns, and an additional lifetime component of 20.57 ns. The calculated  $\lambda_{\text{LR}}$  is 7.986, larger than the critical value 5.991 at the 0.05 significance level. Again, LRT assesses that at the 0.05 significance level, the triexponential decay model better fits the PL decay curve of this trajectory segment than the biexponential decay model. This procedure is repeated on every selected trajectory segment of the bright intensity state, except for the ones containing less than 400 photons to ensure the reliability of fitting results and LRT. It turns out that for a total of 105 analyzed trajectory segments of the QD, 12 of them are better fitted with triexponential decay model at the 0.05 significance level (see details in Table S1). Moreover, these 12 trajectory segments exhibit a common feature, that is, the value of the intermediate lifetime component is about half of the longest lifetime component, which is also observed in previous lifetime blinking studies.<sup>2,3</sup> We thus conclude that lifetime blinking exists in the example QD as well. The whole process is repeated on every QD measured, and the majority of them (35 out of 53) shows very similar results to the example QD (summarized in Table S2). For these QDs, there are typically 10–20% of analyzed trajectory segments that are better fitted with triexponential decay model at the 0.05 significance level, whereas the estimated false-positive rate of LRT at the 0.05 significance level is on the order of 1% (see details in SI Section 6). We therefore confirm that lifetime blinking generally exists in this type of compact CdSe/CdS core/shell QDs.

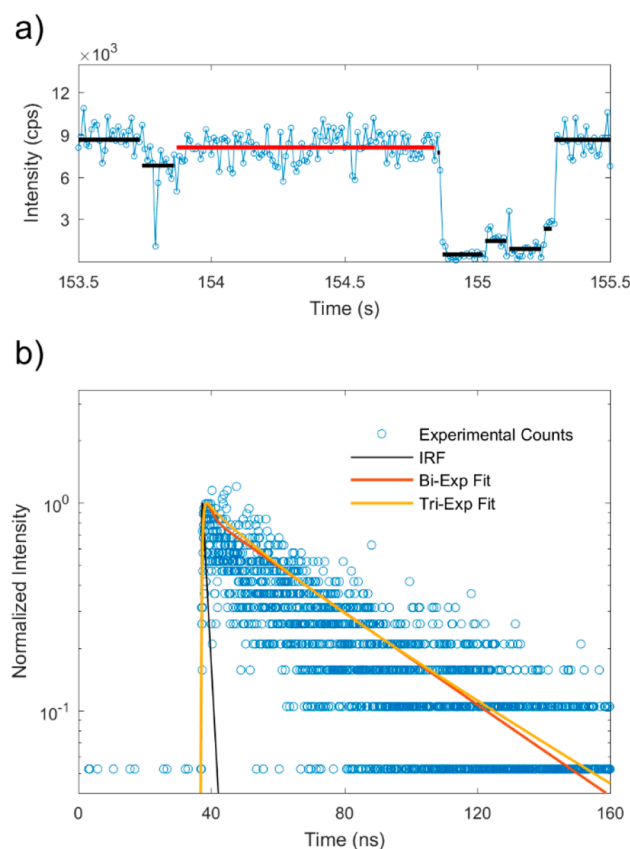


**Figure 3.** (a) An episode of the PL trajectory from Figure 2a. A selected trajectory segment of the bright intensity state is highlighted by the red line. (b) The PL decay data (blue) of the highlighted trajectory segment in (a) is fitted by convoluting IRF (black) with biexponential decay model (red) or triexponential decay model (yellow).

Now that lifetime blinking is confirmed in the compact CdSe/CdS core/shell QDs, a question arises naturally: for a PL trajectory segment identified to have lifetime blinking, does lifetime blinking occur as a single event or multiple events during the trajectory segment? To answer this question, we first assume lifetime blinking occurs as a single event in a trajectory segment of the bright intensity state. Allow  $T$ ,  $T'$  to be the durations of the neutral bright state and lifetime blinking state respectively,  $I$ ,  $I'$  to be the PL intensities of the neutral bright state and lifetime blinking state respectively, and  $N$ ,  $N'$  to be the numbers of photons emitted during the neutral bright state and lifetime blinking state, respectively. The aforementioned autocorrelation analysis indicates that PL intensity is stable during the selected trajectory segments of the bright intensity state, that is,  $I \approx I'$ . Therefore

$$\frac{N'}{N} = \frac{I' \cdot T'}{I \cdot T} \approx \frac{T'}{T} \quad (1)$$

From triexponential fitting results, we assign the shortest and longest lifetime components,  $\tau_1$  and  $\tau_3$ , which correspond to the PL lifetimes of biexciton and exciton to the neutral bright state and assign the intermediate lifetime component  $\tau_2$  to the lifetime blinking state. Obviously

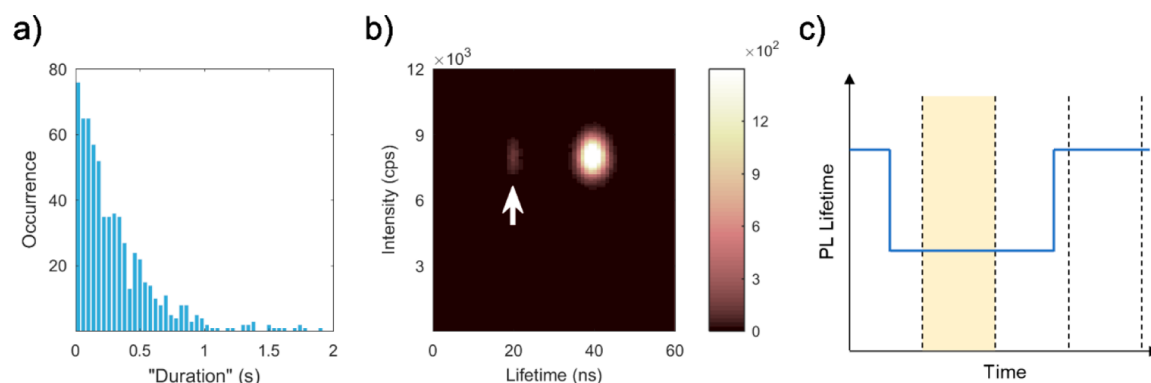


**Figure 4.** (a) Histogram of lifetime blinking durations of all the QDs examined, assuming lifetime blinking occurs as single events in the trajectory segments identified to have lifetime blinking. (b) FLID heatmap constructed from the simulated emission from a single QD with a 50 ms bin time, assuming the durations of lifetime blinking events follow the distribution in (a). The arrow highlights the population that comes from the lifetime blinking state. (c) Scheme of a single lifetime blinking event that lasts longer than twice the bin time. The QD is totally in the lifetime blinking state during the highlighted time bin.

$$\frac{N'}{N} = \frac{\int A_2 \cdot e^{-t/\tau_2} dt}{\int (A_1 \cdot e^{-t/\tau_1} + A_3 \cdot e^{-t/\tau_3}) dt} = \frac{A_2 \cdot \tau_2}{A_1 \cdot \tau_1 + A_3 \cdot \tau_3} \quad (2)$$

The values of lifetime components and their pre-exponential factors are obtained from triexponential fitting. Therefore, the duration of lifetime blinking  $T'$  can be estimated by eqs 1 and 2. For example, the duration of lifetime blinking of the trajectory segment highlighted in Figure 3a is estimated to be  $\sim 0.19$  s assuming it occurs as a single event. Under the single event assumption, we estimate the “durations” of lifetime blinking events of all the QDs that asserted to exhibit the phenomenon. The resultant distribution of lifetime blinking durations is shown in Figure 4a. Although the population of lifetime blinking events decreases as the duration increases, the estimated durations are surprisingly long. Assuming the durations of lifetime blinking follow this distribution, we can simulate the emission from a single QD by a Monte Carlo model (see details in SI Section 7). Applying the typical parameters obtained from the experiments, the FLID heatmap constructed from the simulated single QD emission with a 50 ms bin time is shown in Figure 4b. Highlighted by the arrow, a weak yet distinct population emerges. The intensities of this data point cluster are close to those of the dominant data point cluster, but the lifetimes of this data point cluster are considerably shorter than those of the dominant data point cluster. Apparently, this population comes from the lifetime blinking state. However, this population from simulation is not observed in the FLID of the example QD in Figure 1c, nor is it seen in any FLIDs constructed from the experiments. Hence, the assumption that lifetime blinking occurs as a single event in a PL trajectory segment is not valid. Instead, lifetime blinking generally occurs as multiple events in the selected PL trajectory segments. Accordingly, the durations of single lifetime blinking events are shorter than those estimated under the single event assumption.

Unfortunately, the statistical methods employed in this study cannot pinpoint lifetime blinking events in trajectory segments or determine their exact durations. Nevertheless, here we give a general conservative time scale of the durations of lifetime blinking events in this type of CdSe/CdS core/shell QDs. As shown in Figure 4c, if a single lifetime blinking event can last longer than twice of the bin time used for FLID analysis, there is at least one time bin during which the QD is totally in the

lifetime blinking state, no matter how the PL signals are binned. Multiple lifetime blinking events with such long durations would result in a data point cluster diverging at the lifetime axis from the dominant data point cluster in the FLID, which is never observed in the FLIDs constructed from the experiments. Thus, lifetime blinking events in this type of QDs should typically last shorter than twice of the bin time used for FLID analysis, which is 100 ms ( $50 \text{ ms} \times 2$ ) in this study.

We adopt the framework from previous literature<sup>2</sup> to explain the lifetime blinking mechanism here. Shown in Figure 5, a QD could switch between a neutral state (a) and a charged state (b) via charging and discharging processes after photoexcitation. When a neutral exciton is formed in the core of the QD, the radiative recombination rate is much larger than the intrinsic nonradiative rate, so the PL quantum yield is close to unity, that is, the QD is in the neutral bright state. Note that the QD could still exhibit intensity blinking in the neutral state due to accessing nonradiative recombination pathways such as trapping<sup>19</sup> but that is beyond the scope of this study where we focus on the processes that could lead to lifetime blinking. Charging frequently happens in QDs at the experimental time scale even under low excitation power.<sup>20</sup> A trion in the CdSe core can be formed by processes such as Auger ionization<sup>21</sup> in which a charge is ejected from the core after biexciton formation. The trions formed in CdSe/CdS QDs via photoionization are primarily negative trions.<sup>22,23</sup> A negative trion has two electrons and one hole, as shown in Figure 5b. According to the statistical scaling rule,<sup>24</sup> the radiative recombination rate of a negative trion is doubled compared to that of a neutral exciton. When no additional fast nonradiative processes are activated, the corresponding PL lifetime is roughly half of that of the neutral bright state. Meanwhile, the PL quantum yield is still close to unity. In that case, the QD is in the lifetime blinking state shown in Figure 5c. Conversely, if fast nonradiative processes are activated and the rates are considerably larger than the radiative recombination rate of the negative trion, the PL quantum yield is reduced appreciably. In that case, the QD is in the intensity blinking state shown in Figure 5d.

This is only half of the story. The main difference of lifetime blinking in compact CdSe/CdS core/shell QDs compared to those reported previously is that lifetime blinking events revealed in this study are insignificant and short-lived. This disparity originates from differences in the accessibility and

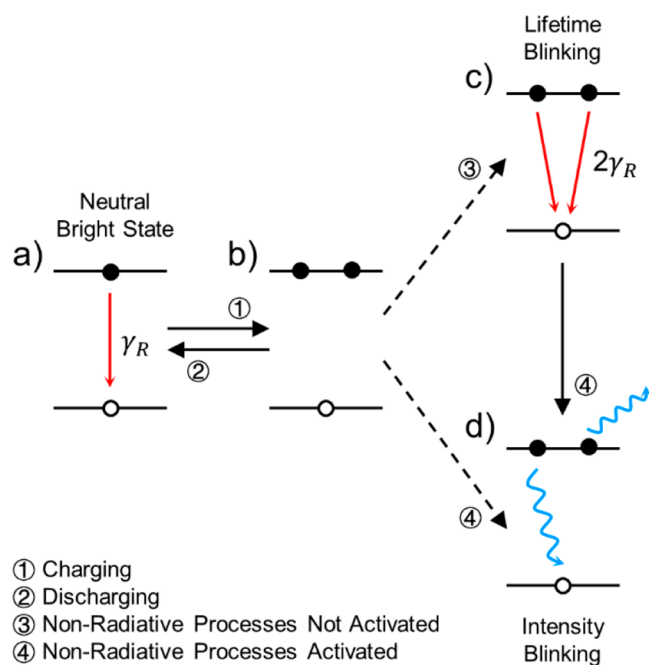


**Figure 5.** Schematic illustration of the physical processes in a QD after photoexcitation. A QD could switch between a neutral state (a) and a charged state (b) via charging and discharging processes. When the QD is neutral, the radiative recombination rate ( $\gamma_R$ ) is much larger than the intrinsic nonradiative rate, so the PL quantum yield is close to unity. When the QD is negatively charged and nonradiative processes are not activated, the resultant radiative recombination rate is doubled ( $2\gamma_R$ ), so the QD is in the lifetime blinking state (c); when the QD is negatively charged and nonradiative processes are activated, it is in the intensity blinking state (d). Lifetime blinking can be terminated by either discharging or activating nonradiative processes.

efficiency of nonradiative processes among QDs with varied crystal structures. For the QDs reported to have long lifetime blinking events, their structures are specially engineered by growing extra thick shells<sup>2</sup> or multiple radially graded interfacial alloy layers.<sup>3</sup> As a result, the nonradiative Auger process is greatly suppressed or slowed down in those QDs, so that its rate is negligible or only comparable to the radiative recombination rate. When such a QD is negatively charged, even though the Auger process activates, the PL intensity is largely unaffected if other nonradiative processes are not involved. Therefore, the lifetime blinking state could last long. Note that other nonradiative processes that lead to PL quenching coexist with the Auger process,<sup>25</sup> so intensity blinking could still occur in those QDs.<sup>3</sup> However, for the CdSe/CdS core/shell QDs examined in this study, the QD volume is only moderate. According to the volume scaling rule,<sup>26</sup> the rate of Auger process is relatively fast. In addition, the less bright states can be frequently observed in the PL intensity trajectory in Figure 1a, which implies that the nonradiative processes are generally efficient. When such a QD is negatively charged, intensity blinking is favored over lifetime blinking. Only under the condition of when charging occurs but nonradiative processes are not activated will ensure a lifetime blinking event. Even if it happens, the lifetime blinking event could easily be terminated.

In this study, we have proven that generally there are multiple lifetime blinking events within one trajectory segment of the bright intensity state. This means, at least after some quick lifetime blinking events, the QD will return to the neutral

bright state due to discharging. More importantly, the charged QD could also switch from the lifetime blinking state to intensity blinking. This type of CdSe/CdS core/shell QDs are quasi type-II semiconductors, where the conduction band offset at the CdSe/CdS interface is considerably smaller than the valence band offset.<sup>27,28</sup> Because of that, after photoexcitation holes are more confined to the core whereas electrons are more delocalized. When a negative trion is formed in the core, two electrons will repel each other due to Coulomb interaction. At room temperature, the electron thermal delocalization could cause electrons to diffuse out of the core.<sup>29,30</sup> During this diffusion process, electrons are likely to access sites that activate efficient nonradiative processes, making the QD switching from the lifetime blinking state to intensity blinking. These sites could be, for example, defects in the shell or at the outer surface. Altogether lifetime blinking can be terminated by either discharging or activation of nonradiative processes. Despite discharging, activation of nonradiative processes is inclined to happen in the compact CdSe/CdS core/shell QDs at room temperature, so the lifetime blinking state is typically short-lived. A potential strategy to lengthen lifetime blinking durations while retaining the compact size of QDs is to sharpen the interfacial potential. By doing that, electrons in such QDs when charged may be confined in the cores from accessing sites that activate nonradiative processes, so the QDs could stay in the lifetime blinking state and maintain high emission intensity.

## CONCLUSIONS

In summary, we use statistical methods to demonstrate that lifetime blinking exists in compact CdSe/CdS core/shell QDs, in which nonradiative processes are efficient when activated. The lifetime blinking events are typically short-lived that they failed to be detected by traditional binning analysis methods. Lifetime blinking only happens when a QD is negatively charged while nonradiative processes are not activated. However, the easy accessibility to efficient nonradiative processes after negative trion formation, along with discharging, leads to the quick termination of lifetime blinking events in the compact CdSe/CdS QDs. The streamline of our analysis methods, dividing a PL trajectory into segments and performing statistical tests on selected segments, may be employed to study fluorescence fluctuations in other materials with statistical significance.

This study not only gives a microscopic understanding of charging-related processes in QDs but also provides an alternative perspective in structural engineering of QDs for desired photophysical properties. For example, in the hope of suppressing intensity blinking to improve the PL quantum yield of QDs, people previously endeavored to smoothen the potential at the interface of QDs to reduce the nonradiative Auger rate.<sup>31</sup> This study suggests that whether intensity blinking or lifetime blinking inclines to happen in a charged QD depends on the accessibility to sites that activate nonradiative processes. Accordingly, a sharp, distinct interfacial potential may not be absolutely detrimental for suppressing intensity blinking, as it would better confine electrons in the core from accessing sites that activate nonradiative processes, therefore preventing intensity blinking to some extent. This assessment is in the opposite direction from the previous efforts of smoothening the interfacial potential. Actually, some recent synthetic advances seem to support this assessment because the synthesized QDs with distinct interfacial potentials

have remarkable PL quantum yields compared to their counterparts with smooth interfacial potentials.<sup>4,32,33</sup> Further systematic studies are needed to evaluate the validity of the assessment.

## ■ ASSOCIATED CONTENT

### Supporting Information

The Supporting Information is available free of charge at <https://pubs.acs.org/doi/10.1021/acs.jpcc.1c03949>.

Synthetic methods, instruments, transmission electron microscopy images, optical spectra, additional single QD data, and details of the data analysis (PDF)

## ■ AUTHOR INFORMATION

### Corresponding Author

Jing Zhao – Institute of Materials Science and Department of Chemistry, University of Connecticut, Storrs Mansfield, Connecticut 06269, United States; [orcid.org/0000-0002-6882-2196](https://orcid.org/0000-0002-6882-2196); Phone: 860-486-2443; Email: [jing.zhao@uconn.edu](mailto:jing.zhao@uconn.edu); Fax: 860-486-2981

### Authors

Yonglei Sun – Institute of Materials Science, University of Connecticut, Storrs Mansfield, Connecticut 06269, United States; [orcid.org/0000-0001-6713-364X](https://orcid.org/0000-0001-6713-364X)

Hua Zhu – Department of Chemistry, Brown University, Providence, Rhode Island 02912, United States

Na Jin – Department of Chemistry, Brown University, Providence, Rhode Island 02912, United States

Ou Chen – Department of Chemistry, Brown University, Providence, Rhode Island 02912, United States;

[orcid.org/0000-0003-0551-090X](https://orcid.org/0000-0003-0551-090X)

Complete contact information is available at: <https://pubs.acs.org/doi/10.1021/acs.jpcc.1c03949>

### Author Contributions

Y.S. and J.Z. conceived the project. H.Z. and N.J. synthesized QDs under the supervision of O.C. Y.S. performed spectroscopic measurements under the supervision of J.Z. Y.S. and J.Z. analyzed the data and wrote the manuscript. All authors contributed to the discussion. All authors have given approval to the final version of the manuscript.

### Notes

The authors declare no competing financial interest.

## ■ ACKNOWLEDGMENTS

The work is partially supported by the National Science Foundation CAREER Award (CHE-1554800). O.C. acknowledges the support from the National Science Foundation CAREER Award (DMR-1943930).

## ■ REFERENCES

(1) Nirmal, M.; Dabbousi, B. O.; Bawendi, M. G.; Macklin, J.; Trautman, J.; Harris, T.; Brus, L. E. Fluorescence Intermittency in Single Cadmium Selenide Nanocrystals. *Nature* **1996**, *383*, 802.

(2) Galland, C.; Ghosh, Y.; Steinbrück, A.; Hollingsworth, J. A.; Htoon, H.; Klimov, V. I. Lifetime Blinking in Nonblinking Nanocrystal Quantum Dots. *Nat. Commun.* **2012**, *3*, 1–7.

(3) Park, Y.-S.; Lim, J.; Makarov, N. S.; Klimov, V. I. Effect of Interfacial Alloying Versus “Volume Scaling” on Auger Recombination in Compositionally Graded Semiconductor Quantum Dots. *Nano Lett.* **2017**, *17*, 5607–5613.

(4) Lee, S. H.; Kim, Y.; Jang, H.; Min, J. H.; Oh, J.; Jang, E.; Kim, D. The Effects of Discrete and Gradient Mid-Shell Structures on the Photoluminescence of Single InP Quantum Dots. *Nanoscale* **2019**, *11*, 23251–23258.

(5) Qin, W.; Guyot-Sionnest, P. Evidence for the Role of Holes in Blinking: Negative and Oxidized CdSe/CdS Dots. *ACS Nano* **2012**, *6*, 9125–9132.

(6) Crouch, C. H.; Sauter, O.; Wu, X.; Purcell, R.; Querner, C.; Drndic, M.; Pelton, M. Facts and Artifacts in the Blinking Statistics of Semiconductor Nanocrystals. *Nano Lett.* **2010**, *10*, 1692–1698.

(7) Pelton, M.; Smith, G.; Scherer, N. F.; Marcus, R. A. Evidence for a Diffusion-Controlled Mechanism for Fluorescence Blinking of Colloidal Quantum Dots. *Proc. Natl. Acad. Sci. U. S. A.* **2007**, *104*, 14249–14254.

(8) Rabouw, F. T.; Antolinez, F. V.; Brechbühler, R.; Norris, D. J. Microsecond Blinking Events in the Fluorescence of Colloidal Quantum Dots Revealed by Correlation Analysis on Preselected Photons. *J. Phys. Chem. Lett.* **2019**, *10*, 3732–3738.

(9) Köllner, M.; Wolfrum, J. How Many Photons Are Necessary for Fluorescence-Lifetime Measurements? *Chem. Phys. Lett.* **1992**, *200*, 199–204.

(10) Chen, O.; Zhao, J.; Chauhan, V. P.; Cui, J.; Wong, C.; Harris, D. K.; Wei, H.; Han, H.-S.; Fukumura, D.; Jain, R. K.; et al. Compact High-Quality CdSe-CdS Core-Shell Nanocrystals with Narrow Emission Linewidths and Suppressed Blinking. *Nat. Mater.* **2013**, *12*, 445.

(11) Messin, G.; Hermier, J.-P.; Giacobino, E.; Desbiolles, P.; Dahan, M. Bunching and Antibunching in the Fluorescence of Semiconductor Nanocrystals. *Opt. Lett.* **2001**, *26*, 1891–1893.

(12) Bae, Y. J.; Gibson, N. A.; Ding, T. X.; Alivisatos, A. P.; Leone, S. R. Understanding the Bias Introduced in Quantum Dot Blinking Using Change Point Analysis. *J. Phys. Chem. C* **2016**, *120*, 29484–29490.

(13) Watkins, L. P.; Yang, H. Detection of Intensity Change Points in Time-Resolved Single-Molecule Measurements. *J. Phys. Chem. B* **2005**, *109*, 617–628.

(14) Li, H.; Yang, H. Statistical Learning of Discrete States in Time Series. *J. Phys. Chem. B* **2019**, *123*, 689–701.

(15) Wahl, M.; Gregor, I.; Patting, M.; Enderlein, J. Fast Calculation of Fluorescence Correlation Data with Asynchronous Time-Correlated Single-Photon Counting. *Opt. Express* **2003**, *11*, 3583–3591.

(16) Cui, J.; Beyler, A. P.; Bischof, T. S.; Wilson, M. W.; Bawendi, M. G. Deconstructing the Photon Stream from Single Nanocrystals: From Binning to Correlation. *Chem. Soc. Rev.* **2014**, *43*, 1287–1310.

(17) Achermann, M.; Hollingsworth, J. A.; Klimov, V. I. Multiexcitons Confined within a Subexcitonic Volume: Spectroscopic and Dynamical Signatures of Neutral and Charged Biexcitons in Ultrasmall Semiconductor Nanocrystals. *Phys. Rev. B: Condens. Matter Mater. Phys.* **2003**, *68*, 245302.

(18) Caruge, J.-M.; Chan, Y.; Sundar, V.; Eisler, H.; Bawendi, M. G. Transient Photoluminescence and Simultaneous Amplified Spontaneous Emission from Multiexciton States in CdSe Quantum Dots. *Phys. Rev. B: Condens. Matter Mater. Phys.* **2004**, *70*, 085316.

(19) Rosen, S.; Schwartz, O.; Oron, D. Transient Fluorescence of the Off State in Blinking CdSe/CdS/ZnS Semiconductor Nanocrystals Is Not Governed by Auger Recombination. *Phys. Rev. Lett.* **2010**, *104*, 157404.

(20) Peterson, J. J.; Nesbitt, D. J. Modified Power Law Behavior in Quantum Dot Blinking: A Novel Role for Biexcitons and Auger Ionization. *Nano Lett.* **2009**, *9*, 338–345.

(21) Efron, A. L.; Rosen, M. Random Telegraph Signal in the Photoluminescence Intensity of a Single Quantum Dot. *Phys. Rev. Lett.* **1997**, *78*, 1110.

(22) Galland, C.; Ghosh, Y.; Steinbrück, A.; Sykora, M.; Hollingsworth, J. A.; Klimov, V. I.; Htoon, H. Two Types of Luminescence Blinking Revealed by Spectroelectrochemistry of Single Quantum Dots. *Nature* **2011**, *479*, 203–207.

- (23) Melnychuk, C.; Guyot-Sionnest, P. Multicarrier Dynamics in Quantum Dots. *Chem. Rev.* **2021**, *121*, 2325–2372.
- (24) Klimov, V. I.; McGuire, J.; Schaller, R. D.; Rupasov, V. Scaling of Multiexciton Lifetimes in Semiconductor Nanocrystals. *Phys. Rev. B: Condens. Matter Mater. Phys.* **2008**, *77*, 195324.
- (25) Yuan, G.; Gómez, D. E.; Kirkwood, N.; Boldt, K.; Mulvaney, P. Two Mechanisms Determine Quantum Dot Blinking. *ACS Nano* **2018**, *12*, 3397–3405.
- (26) Robel, I.; Gresback, R.; Kortshagen, U.; Schaller, R. D.; Klimov, V. I. Universal Size-Dependent Trend in Auger Recombination in Direct-Gap and Indirect-Gap Semiconductor Nanocrystals. *Phys. Rev. Lett.* **2009**, *102*, 177404.
- (27) Peng, X.; Schlamp, M. C.; Kadavanich, A. V.; Alivisatos, A. P. Epitaxial Growth of Highly Luminescent CdSe/CdS Core/Shell Nanocrystals with Photostability and Electronic Accessibility. *J. Am. Chem. Soc.* **1997**, *119*, 7019–7029.
- (28) Pietryga, J. M.; Park, Y.-S.; Lim, J.; Fidler, A. F.; Bae, W. K.; Brovelli, S.; Klimov, V. I. Spectroscopic and Device Aspects of Nanocrystal Quantum Dots. *Chem. Rev.* **2016**, *116*, 10513–10622.
- (29) Javaux, C.; Mahler, B.; Dubertret, B.; Shabaev, A.; Rodina, A.; Efros, A. L.; Yakovlev, D.; Liu, F.; Bayer, M.; Camps, G.; et al. Thermal Activation of Non-Radiative Auger Recombination in Charged Colloidal Nanocrystals. *Nat. Nanotechnol.* **2013**, *8*, 206–212.
- (30) Shabaev, A.; Rodina, A.; Efros, A. L. Fine Structure of the Band-Edge Excitons and Trions in CdSe/CdS Core/Shell Nanocrystals. *Phys. Rev. B: Condens. Matter Mater. Phys.* **2012**, *86*, 205311.
- (31) Bae, W. K.; Padilha, L. A.; Park, Y.-S.; McDaniel, H.; Robel, I.; Pietryga, J. M.; Klimov, V. I. Controlled Alloying of the Core-Shell Interface in CdSe/CdS Quantum Dots for Suppression of Auger Recombination. *ACS Nano* **2013**, *7*, 3411–3419.
- (32) Park, J.; Jayaraman, A.; Wang, X.; Zhao, J.; Han, H.-S. Nanocrystal Precursor Incorporating Separated Reaction Mechanisms for Nucleation and Growth to Unleash the Potential of Heat-up Synthesis. *ACS Nano* **2020**, *14*, 11579–11593.
- (33) Cao, H.; Ma, J.; Huang, L.; Qin, H.; Meng, R.; Li, Y.; Peng, X. Design and Synthesis of Antiblinking and Antibleaching Quantum Dots in Multiple Colors Via Wave Function Confinement. *J. Am. Chem. Soc.* **2016**, *138*, 15727–15735.